Computer Simulations of the Atmospheric Chemistry of Sulfate and Nitrate Formation

Abstract. *Simulations of the atmospheric chemistry of sulfate and inorganic nitrate formation have been carried out by means of a detailed gas phase–liquid phase chemical kinetic mechanism. Consideration has been given to the effect of changes in sulfur dioxide, nitrogen oxides, and reactive hydrocarbon concentrations on sulfate and nitrate formation for conditions typical of the midwestern and northeastern United States. The results indicate significant nonlinearities in the chemistry of acid formation, particularly between sulfur dioxide and sulfate concentrations.*

Evidence of lake acidification in northern America and Scandinavia has been reported in recent years. It appears that mitigation of the acid deposition problem will require a reduction in the ambient concentrations of sulfate and nitrate brought about through control of their rate of formation in the atmosphere (*1*). However, because of the complex nonlinear aspects of atmospheric chemistry, reductions in the concentrations of the anthropogenic precursors sulfur dioxide (SO_2) and nitrogen oxides (NO_x) may not lead to equivalent reductions in sulfate and nitrate concentrations, respectively. In addition, the reaction of reactive hydrocarbons (RHC) with NO_x determines the ambient concentrations of oxidants in the atmosphere; therefore, SO_2 and NO_x oxidation rates are also sensitive to RHC concentrations.

This report presents the results of simulations of the atmospheric chemistry of sulfate and nitrate formation performed to investigate the effect of changes in SO_2, NO_x, and RHC concentrations on sulfate and nitrate concentrations for conditions typical of midwestern and northeastern America. Our model calculations suggest that there are strong nonlinearities in the atmospheric chemistry of acid species.

The mathematical model used for this investigation provides a detailed treatment of the chemistry of 54 chemical species including sulfate, nitrate, SO_2, NO_x, RHC, O_3, and H_2O_2 in the gas phase and in cloud droplets (*2*). The following major reactions lead to acid formation in the gas phase (*3, 4*):

$$SO_2 + OH(+ O_2, H_2O) \rightarrow H_2SO_4 + HO_2 \quad (1)$$

$$NO_2 + OH \rightarrow HNO_3 \quad (2)$$

$$NO_2 + NO_3 \leftrightarrows N_2O_5 \quad (3a)$$

$$N_2O_5 + H_2O \rightarrow 2\ HNO_3 \quad (3b)$$

The hydrolysis of N_2O_5 (Eq. 3b) is believed to occur both in the gas phase and on droplet surfaces. Gas phase–liquid phase equilibria are treated according to Henry's law, and it is assumed that mass transfer between the gas and liquid phases is limited by the liquid-phase chemical reaction rates (*5*). However, sulfuric acid and radicals, because of their low saturation vapor pressure, are assumed to be transferred from the gas phase to the liquid phase by a diffusion-limited process. The scavenging efficiency of radicals by droplets is assumed to be 1 percent.

The following major reactions lead to acid formation in the liquid phase (*6*):

$$S(IV) + O_3 \rightarrow S(VI) + O_2 \quad (4)$$

$$S(IV) + H_2O_2 \rightarrow S(VI) + H_2O \quad (5)$$

$$S(IV) + \frac{1}{2}O_2 \xrightarrow{Fe^{3+},\ Mn^{2+}} S(VI) \quad (6)$$

Species S(IV) and S(VI) represent two different sulfur oxidation states corresponding to SO_2 (H_2SO_3, HSO_3^-, and SO_3^{2-}) and sulfate (H_2SO_4, HSO_4^-, and SO_4^{2-}), respectively. The reaction rate of Eq. 4 decreases as the *p*H decreases; this oxidation pathway is therefore self-limiting. The reaction rate of Eq. 5 increases as the *p*H decreases; however, this reaction may be oxidant-limited. The oxidation of S(IV) catalyzed by trace metals (Eq. 6) is zero-order with Mn^{2+} and first-order with Fe^{3+}, and synergism may occur when both metals are present.

The model does not treat turbulent diffusion and is therefore representative of a well-mixed atmosphere with uniformly distributed emission sources. Model simulations were conducted for

Table 1. Initial concentrations and emission fluxes used in the model simulations.

Species	Initial concentrations (ppm)		Emission fluxes (mol · m^{-2} year^{-1})
	June simulations	December simulations	
Sulfate	0.00025	0.00005	
Nitrate	0.0005	0.0001	
SO_2	0.010	0.010	0.45
NO_x	0.006	0.006	0.27
RHC	0.015	0.015	0.68
NH_3	0.001	0.001	
H_2O_2*	0.001	0.0001	
O_3	0.045	0.045	
CO_2	320	320	

*0 ppm for gas-phase simulations because the chemical kinetic mechanism calculates H_2O_2 formation during the course of the simulation.

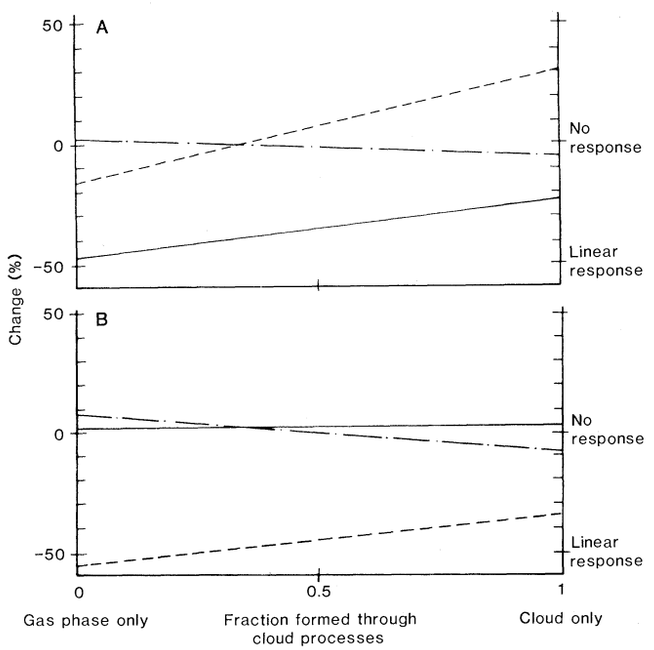

Fig. 1. (A) Percentage change in sulfate formation due to a 50 percent reduction in the SO_2 (——), NO_x (– – –), or reactive hydrocarbon (RHC) (– · –) concentration. (B) Percentage change in nitrate formation due to a 50 percent reduction in the SO_2 (——), NO_x (– – –), or RHC (– · –) concentration.

daytime conditions only so that the assumption of a well-mixed atmosphere would apply. Cloud model simulations were representative of stratus clouds rather than cumulus clouds because the latter require treatment of dry-air entrainment. Therefore, this study considers two extreme cases of atmospheric conditions: dry gas-phase chemistry and cloud chemistry without dry-air entrainment.

Limited data bases exist for the evaluation of a cloud chemistry model. We evaluated the ability of the model to reproduce the major features of atmospheric cloud chemistry by comparing the model calculations with several sets of ambient measurements collected under various conditions. Such comparisons were conducted for nonprecipitating clouds in the Adirondacks, raining clouds in the Ohio River Valley, and nighttime fog and stratus clouds in the Los Angeles Basin. The model calculations were in good agreement with observed concentrations of sulfate, nitrate, and cloud *p*H within the range of experimental uncertainties (*2*).

Four simulations typical of conditions in the midwestern and northeastern United States were conducted: simulation of the atmospheric boundary layer without clouds and simulation of an elevated stratus-cloud layer, each for two sets of seasonal conditions, June and December. Boundary-layer simulations were conducted for a 12-hour period from 0600 to 1800 hours. Cloud-layer simulations were conducted for a 3-hour period from 1000 to 1300 hours since cloud lifetime is a few hours. Dry deposition on the ground was treated for the cloud-free simulations with deposition velocities of 1 cm sec^{-1} for gases and 0.1 cm sec^{-1} for aerosols. Thermodynamic and kinetic parameters were calculated for a temperature of 25°C for all simulations. The temperature dependence of these parameters could easily be incorporated into the calculations to investigate the sensitivity of modeling results to temperature (for example, for seasonal variations). The cloud water content selected for the cloud simulations was 0.5 g m^{-3}. The June and December simulations investigated the effect of solar irradiation on chemical kinetics. Table 1 presents the initial conditions and emission rates used in these four simulations.

The concentrations of SO_2, NO_x, and RHC were independently reduced by 50 percent for each of the four scenarios. These reductions applied to both initial concentrations and emissions. Table 2 presents changes in the amounts of sulfate and inorganic nitrate formed as a result of changes in the precursor concentrations for each simulation. The net effect of a 50 percent reduction in precursor concentrations on acid formation depends on the relative contribution of the clear-sky and stratus-cloud processes to acid species formation. This is illustrated in Fig. 1, A and B, for sulfate and nitrate, respectively.

Table 2. Model simulation results. Changes in sulfate and inorganic nitrate concentrations (percent) due to reductions in precursor concentrations.

Variable	50 percent reduction in					
	SO_2		NO_x		RHC	
	June	December	June	December	June	December
Clear-sky environment						
Sulfate	−48	−48	−18	−9	+9	−9
Nitrate	+1	0	−55	−58	+11	+4
Stratus-cloud environment						
Sulfate	−22	−26	+30	+33	−7	−5
Nitrate	0	+2	−41	−32	−9	−9

Model calculations suggest that the relation between sulfate and SO_2 reduction is nearly linear in a cloud-free atmosphere but is strongly nonlinear if clouds are present. In the latter case, sulfate formation occurs primarily in the liquid phase through the reaction of dissolved SO_2 with H_2O_2 and O_3 (Eqs. 4 and 5). The net effect of SO_2 reduction on sulfate formation depends on the relative contributions of dry gas-phase and cloud processes (Fig. 1A). For example, if we assume that cloud processes account for 50 percent of sulfate formation, a 50 percent reduction in SO_2 concentrations leads to a 36 percent reduction in sulfate (*7*). Reductions in SO_2 concentrations have a negligible effect on nitrate formation.

Our model calculations show that a reduction in NO_x concentrations leads to a decrease in nitrate formation; this decrease is more important for dry gas-phase conditions than in the presence of clouds. A reduction in NO_x emissions leads to a slight reduction in sulfate formation for dry gas-phase conditions but to a significant increase in sulfate formation in the presence of clouds. This results from the effect of changes in NO_x concentrations on oxidant concentrations.

Calculations indicate that a 50 percent reduction in RHC could lead to either a slight increase or a slight decrease in sulfate and nitrate formation, depending on both the season and the occurrence of cloud chemistry (Table 2 and Fig. 1).

In summary, our model calculations suggest that, for the conditions considered, reductions in SO_2 and NO_x lead to nearly equivalent reductions in sulfate and nitrate, respectively, for clear-sky conditions; however, such reductions lead to significantly less reduction in acid levels in the presence of clouds. Changes in RHC do not seem to have significant effects on acid concentrations.

One should view these calculations as illustrative of atmospheric chemistry, recognizing that treatment of atmospheric transport is required for a more accurate determination of the relations between atmospheric acid concentrations and their precursors. For example, entrainment of air into clouds would yield higher oxidant concentrations than those calculated in our cloud simulations and might lead to less nonlinearity between SO_2 and sulfate concentrations. Refinements of the chemical mechanism may also be required as our knowledge of atmospheric chemistry improves. Nevertheless, because the model reported here is based on a detailed treatment of gas-phase and liquid-phase chemistries, it may therefore be considered an effective tool for the analysis of atmospheric acid formation.

CHRISTIAN SEIGNEUR
PRADEEP SAXENA, PHILIP M. ROTH
Systems Applications, Inc.,
101 Lucas Valley Road,
San Rafael, California 94903

References and Notes

1. National Research Council, *Acid Deposition—Atmospheric Processes in Eastern North America* (National Academy Press, Washington, D.C., 1983).
2. C. Seigneur, P. Saxena, P. M. Roth, in *Air Pollution Modeling and Its Applications*, C. de Wispelaere, Ed. (Plenum, New York, in press), vol. 4; C. Seigneur and P. Saxena, *Atmos. Environ.*, in press.
3. J. G. Calvert and W. R. Stockwell, *Environ. Sci. Technol.* **17**, 428A (1983).
4. L. W. Richards, *Atmos. Environ.* **17**, 397 (1983).
5. L. B. Baboolal, H. R. Pruppacher, J. H. Topalian, *J. Atmos. Sci.* **38**, 856 (1981); S. E. Schwartz and J. E. Freiberg, *Atmos. Environ.* **15**, 1129 (1981).
6. L. R. Martin, in *SO_2, NO and NO_2 Oxidation Mechanisms*, J. G. Calvert, Ed. (Butterworth, Boston, 1984), pp. 63–100.
7. This fraction of sulfate and nitrate formed in clouds is used as an illustration. For reference, it has been estimated that 70 percent of sulfate is removed by wet deposition [G. M. Hidy, R. C. Henry, D. A. Hansen, K. Ganesan, J. Collins, *Document P-B538-R* (Environmental Research and Technology, Inc., Westlake Village, Calif.,

1983)]. However, some of that sulfate is formed in the dry gas-phase prior to cloud formation.

8. We thank the project officers, R. L. Kerch of Consolidation Coal Company and J. Wootten of Peabody Coal Company, for their continuous support and interest in this work. We also thank V. A. Mohnen for giving helpful advice on the model input data and for providing the measurements obtained by the research group at Whiteface Mountain. We acknowledge the meticulous technical editing provided by J. Rodich and C. Lawson. This study was sponsored by the Consolidation Coal Company and the Peabody Coal Company.

17 January 1984; accepted 3 May 1984

Disruption of the Terrestrial Plant Ecosystem at the Cretaceous-Tertiary Boundary, Western Interior

Abstract. *The palynologically defined Cretaceous-Tertiary boundary in the western interior of North America occurs at the top of an iridium-rich clay layer. The boundary is characterized by the abrupt disappearance of certain pollen species, immediately followed by a pronounced, geologically brief change in the ratio of fern spores to angiosperm pollen. The occurrence of these changes at two widely separated sites implies continentwide disruption of the terrestrial ecosystem, probably caused by a major catastrophic event at the end of the period.*

Since the discovery of an anomalously high concentration of iridium and other platinum-group elements in rocks at the Cretaceous-Tertiary (K/T) boundary at Gubbio, Italy (*1*), over 50 more localities worldwide with anomalously high Ir concentrations have been found in marine rocks at the K/T boundary, as defined by pronounced changes in the marine fossil biota (*2, 3*). We report high Ir anomalies in continental rocks deposited in fluvial environments at the palynologically defined K/T boundary from 12 localities in the Raton Basin in Colorado and New Mexico and two more in the Hell Creek, Montana, area.

The K/T boundary, as defined palynologically, occurs in the lower coal zone of the Raton Formation of Cretaceous and Paleocene age (*4–7*). It lies at the top of a 1- to 2-cm-thick kaolinite-rich clay bed in an ordinary-appearing interval of carbonaceous shale and coal (Fig. 1). The first determination of the approximate position of the palynological boundary was described by Orth *et al.* (*4*). This boundary is defined by the disappearance of several Cretaceous palynomorph taxa, chiefly *Proteacidites* spp. and *Tilia wodehousei* sensu Anderson, and often *Trisectoris* and *Trichopeltinites*. These taxa have not been found in samples overlying the boundary clay layer.

The disappearance of the taxa did not involve all of the plants represented by the Cretaceous palynomorph assemblage. Although the flora was decimated, some taxa apparently withstood the boundary event only to disappear during the early Paleocene (*Kurtzipites*); a few others have persisted to the present, relatively unchanged (*Ulmipollenites*).

The abrupt increase in the proportions of fern spores to angiosperm pollen at the palynological K/T boundary (*4*) may indicate a local abundance of fern plants at or near the deposition site or, if consistent and widespread, fern-spore dominance could reflect a pronounced change in the regional flora. We now also report fern-spore abundance peaks in samples from Brownie Butte and Seven Blackfoot Creek localities (Hell Creek, Montana) more than 1000 km to the north; the samples were taken immediately above the palynological K/T boundary and the Ir-rich clay layer (*8*). The genera found in the Tertiary fern-spore abundance peaks are also present in terminal Cretaceous rocks as well as in other nearby localities (*9*).

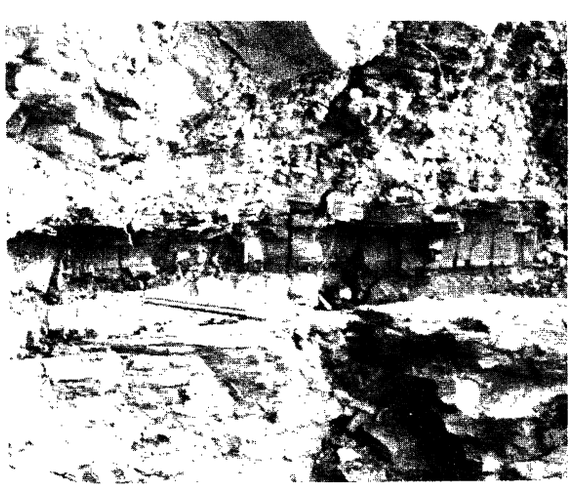

Fig. 1. Photograph of the K/T boundary interval at the Starkville North site near Trinidad, Colorado (*6*). The fossil-pollen-defined boundary is at the top of a white-weathering, kaolinitic claystone bed beneath the dark coal layer. The claystone consists of finely crystalline to amorphous kaolinite with scattered fragments of quartz and feldspar. It contains abundance anomalies of Ir (6 ng/g) and other elements, including Sc, Ti, V, Cr, and Sb, that distinguish it from other nonboundary kaolinitic clay beds that occur in coaly sequences (*14*). A thin, flaky, dark shale separates the kaolinitic claystone from the overlying thin coal bed.

Figure 2 shows the succession of rock types across the boundary in the representative Raton Basin section (the Starkville North site) (*6*). Observations of slides prepared from samples spanning the boundary reveal changes not only in the palynomorph content but also in the kind and abundance of accessory material present. The description below refers to the sampling intervals shown in Fig. 2 but generally represents the boundary interval throughout the Raton Basin.

In the lower part of the section, the samples from Cretaceous carbonaceous shales and shales with coal streaks commonly yield an abundance of cuticular material and epidermal tissue along with a suite of Cretaceous palynomorphs. Palynomorphs are sparse in the overlying boundary clay layer, but there are sufficient specimens to identify the assemblage and determine the fern-spore and angiosperm-pollen percentages. Even when the sample is dark, with an admixture of organic matter, palynomorphs are exiguous. The organic material commonly consists of sapropel and fragmented organic particles.

The overlying thin shale layer also contains scant palynomorphs. The flecks of organic material in this layer are often dark charcoal-like woody tissue consisting of fusinite and semifusinite. Fragmental particles of unidentifiable organic material commonly are present and, occasionally, a few algal spores are observed. The identifiable palynomorphs commonly are fern spores. In this layer, the first evidence of fern-spore dominance appears. The content of fern spores in latest Cretaceous samples from the Raton Basin varies from a few percent to a maximum of about 25 percent. Immediately above the palynological K/T boundary the proportion of fern spores increases to between 65 and 100 percent. For example, the fern-spore component of the assemblage shown in Fig. 2 changes abruptly within less than a centimeter from about 20 to almost 100 percent. This fern-spore dominance immediately above the boundary is present in all Raton Basin K/T boundary localities examined where Ir anomalies have been found. Fern-spore dominance is generally not associated with other thin ash falls